Experimental and Numerical Nonequilibrium Flow Studies

J. H. SPURK*
U. S. Army Ballistic Research Laboratories, Aberdeen Proving Ground, Md.

Experimental and numerical studies of the nonequilibrium shock layer around cones in hypersonic pure oxygen flows are reported. Experimental conditions are such that rotational, vibrational, and dissociation relaxation occur simultaneously. Attention is given to the effect of coupled relaxation on the flow properties in the shock layer. The phenomenological models of Hammerling et al., and Treanor and Marrone predict the flowfield qualitatively correct. However, quantitative differences in shock geometry and density distribution are appreciable. Better quantitative agreement with experiment is reached if in these models a temperature dependent efficiency of O_2 and O in the relaxation processes is assumed.

Introduction

FOR certain flight conditions, the flowfield around the body is to a large extent determined by the rate with which various relaxation processes occur. In the past much effort has been devoted to the numerical prediction of these flowfields. The analysis assumes a gas model by specifying the relaxation equations and the equations of state. The most commonly used gas models assume only one relaxation process with equilibrium or frozen conditions existing for the remaining internal modes. This appreciable simplification is possible if the relaxation times characterizing the various relaxation processes are vastly different, with the relaxation time of the dominant process in the order of the flow time L/U_∞. For example, the gas model which assumes translational, rotational, and vibrational equilibrium, frozen ionization, and which considers as the only relaxation processes dissociation and recombination, has been widely used[1-3] even outside its range of applicability to predict the flowfields around bodies in hypersonic flight. Such a model is only valid in a regime where the inequalities $\tau_{tr} < \tau_{rot} < \tau_{vib} \ll \tau_{diss} \ll \tau_{ion}$ hold and where $\tau_{diss} \sim 0(L/U_\infty)$. Experimental studies[4] of the flowfield around cones have confirmed the adequacy of this model for these conditions. For a temperature above 8000°K in the shock layer the preceding inequalities cease to be valid for the oxygen component, and simultaneous vibrational and dissociation relaxation occur. The two processes interact with each other, so that the over-all relaxation is largely affected.

Phenomenological rate equations[5] accounting for the vibration dissociation coupling have been used to compute the reaction profiles behind strong normal shocks in air. Comparison with experimental data[6] in terms of half-decomposition distance of the oxygen component shows the experimental distance to be substantially larger than the theoretical value. For the case of interest here, i.e., the hypersonic flow around a body, departure of experiments from prediction should be expected all the more, because the relaxation process is additionally affected by the gas dynamic process.

It is the purpose of this paper to report experimental data on the shock layer flow for freestream conditions where considerable coupling between rotation, vibration, and dissociation exists, their respective relaxation times being of the same order of magnitude when extrapolated to the condition of the experiments. The experimental results are compared with numerical prediction of the flowfield. Since at present there is no theory to describe this coupled relaxation process, the gas models on which the computations are based are simplified in various respects; mainly one or several of the pertinent relaxation times are assumed zero or infinite.

The test gas was pure oxygen rather than air to avoid additional complexities associated with a mixture of diatomic gases. On the other hand, the significant effects of relaxation under nonisothermal conditions are preserved. Oxygen is a good choice for the present purpose because its reaction kinetics have been most extensively studied.

Experiments

The hypersonic high-energy flow of pure oxygen is generated in an expansion tube.[7] The expansion tube for one of the experiments is operated in such a manner as to avoid any freestream dissociation, i.e., the compressibility $Z_\infty = 1$.

In this case, subsequently referred to as case 1, the freestream condition is determined by the measurement of freestream density and freestream pressure. The freestream vibrational energy may be somewhat higher than indicated by the translational temperature $T_\infty = p_\infty(\rho_\infty R)^{-1}$. For the other experiment (case 2) the expansion tube is operated in the reflected mode; this may result in a freestream nonequilibrium condition with $Z_\infty \sim 1.1$ where neither the state of dissociation nor the vibrational energy is in equilibrium with the translational temperature. The freestream density measurement is made by streak interferometry. The accuracy of this measurement is affected by two errors: the random error in measuring the fringe shift, which is about 10%, and a systematic error resulting from the fact that the light beam traverses the boundary layer on the observation windows of the expansion tube.[8] The latter error can be corrected in an approximate way. The combined error is not larger than 20% and measured freestream density is adjusted within this bound as described in the section entitled Comparison of Numerical and Experimental Data. Impurity concentrations in the shock layer have been measured for conditions similar to the condition of these experiments. The concentration of the main contaminants Fe, Cr, CN was found to be less than 400 ppm.[9] The test gas prior to admission into the facility has been checked for nitrogen contamination, which was found to be less than 10 ppm. For the actual test, the gas is at relatively high pressure ($\sim\frac{1}{2}$ Atm) so that contamination by residual air in the tube (50μ Hg) is small. These impurity concentrations are too small to affect the relaxation process especially at the high shock layer temperatures of these experiments.

The main experimental tool is a Mach-Zehnder optical interferometer which is used to observe, without interference,

Presented as Paper 69-136 at the AIAA 7th Aerospace Sciences Meeting, New York, January 20–22, 1969; submitted January 29, 1969; revision received November 20, 1969. The author wishes to extend his appreciation to the people that helped in obtaining the data given here, especially B. Bilsborough, J. Bartos, and N. Gerber.

* Chief, Fluid Dynamics Branch, Exterior Ballistics Laboratory. Associate Fellow AIAA.

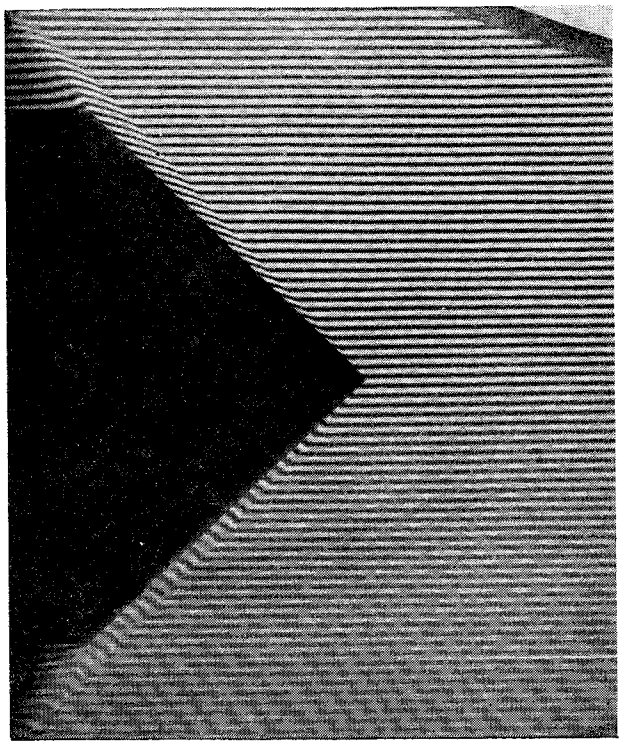

Fig. 1 Frame interferogram of a hypersonic flow around a cone. Case 1, observing wavelength: λ = 4358 Å, freestream conditions: U_∞ = 6350 m/sec, ρ_∞ = 0.0148 kg/m³, p_∞ = 4810 N/m².

the stationary flow around the model and the freestream flow. The frame interferograms of the two flowfields are shown in Figs. 1 and 2. The model diameter is 2 in. in both cases, the cone angles 45° and 35°, respectively.

From these interferograms one can determine the shock position and the fringe shift, i.e., the difference of ordinates of the undisturbed and the disturbed fringe in an x;r coordinate system attached to the apex of the cone. x is measured along the axis of the cone and r normal to x (Fig. 3). It is convenient to measure the fringe shift along traces x = const and to present the data as a function of the distance r from the axis along x = const. The actual measurement of the fringe shift is done automatically on a fringe reader; the shock position is measured manually on the same instrument. The fringe reader is essentially a microscope in conjunction with a light sensitive cell. The position of the fringes is found from the variation in back light intensity as the interferogram is scanned. The experimental fringe shift and shock shape are the principal data which are used in the comparison with numerical predictions.

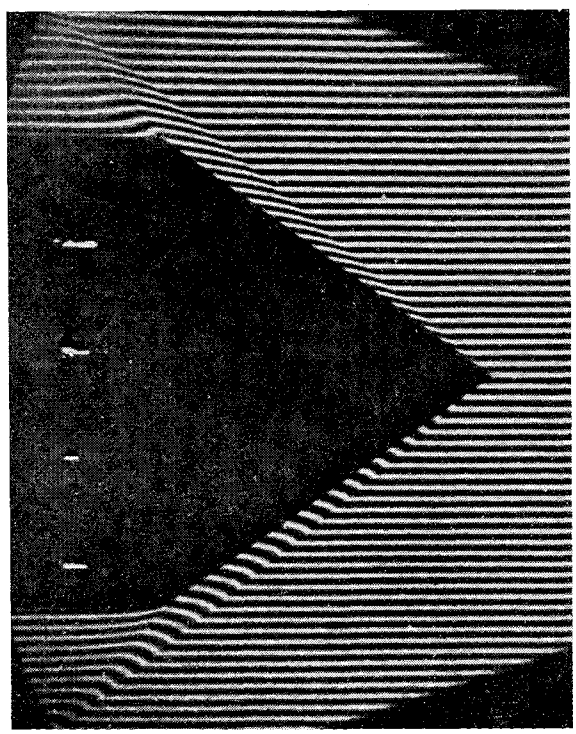

Fig. 2 Frame interferogram of a hypersonic flow around a cone. Case 2, observing wavelength: λ = 5461 Å, freestream conditions: U_∞ = 5710 m/sec, ρ_∞ = 0.0194 kg/m³, p_∞ = 5720 N/m².

Numerical Computations

For the freestream conditions of the experiments, the flow around the conical bodies is purely supersonic and the method of characteristics can be used to integrate numerically the equations of motion together with the rate equations. Once a gas model is specified the integration is rather routine; however, care must be taken to insure reliability of the numerical results. The correctness of the characteristic solution can be judged by comparing its behavior to the simpler conical flow solution of frozen and equilibrium flows. The stream function on the body is computed for each advance in right-running characteristic. The stream function at the body is found by integration along the characteristic from the shock to the body. Since continuity requires zero stream function at the body, the grid size is adjusted in such a way as to keep the value of the stream function on the body to less than 1% of its value at the shock for the same characteristic. More detail on the numerical procedure and on other checks to ascertain the accuracy of the numerical results can be found in Ref. 3.

From the numerical solution the shock position is, of course, known; the fringe shift is then computed along traces x = const using the density and species concentrations along this line and known values of the specific refractivity for each species. This provides the theoretical data for comparison with the experimental data.

Gas Models

The oxygen in the shock layer is assumed to be a mixture of perfect gases: molecular and atomic oxygen. The caloric equation of state includes the contribution of the low-lying electronic states to the energy of the gas, which is then made up of contributions from translation, rotation, vibration, and electronic excitation. The vibrational energy is computed on the basis of an anharmonic oscillator.[10] Ionization may be neglected for the present conditions.

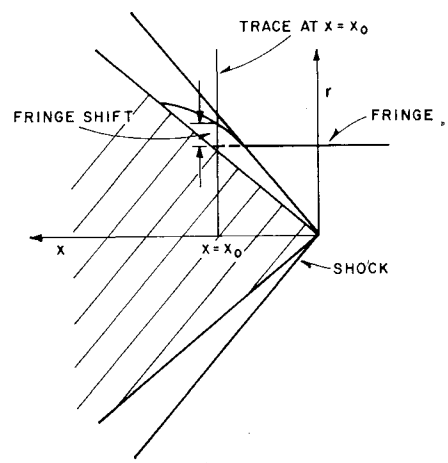

Fig. 3 Sketch illustrating the coordinate system.

For all the computations made the translational and rotational degrees of freedom are assumed to come into equilibrium within the shock, which is considered a surface of discontinuity. Thus, $\tau_{tr} = \tau_{rot} = 0$ for all computations. The rotational relaxation time, though smaller than the vibrational relaxation time, is of the same order for parts of the shock layer. It is well to keep in mind that rotation and possibly translation may not have relaxed to a Boltzmann distribution when vibrational relaxation sets in.

The electronic relaxation time $\tau_{el} = 0$ for all computation, i.e., the population of the electronic levels is based on the translational temperature. There is evidence that the population of the electronic levels follows the vibrational temperature. However, as sample computations show, the effect of electronic excitation on the flowfield is quite small, so that either choice should be adequate.

When the relaxation times go to the limit zero or infinity, the flowfield becomes self similar. Three types of conical flows were computed, which result from the following conditions:

$$\tau_{trans} = \tau_{rot} = \tau_{el} = 0, \qquad \tau_{vib} = \tau_{diss} = \infty \tag{1}$$

$$\tau_{trans} = \tau_{rot} = \tau_{el} = \tau_{vib} = 0, \qquad \tau_{diss} = \infty \tag{2}$$

$$\tau_{trans} = \tau_{rot} = \tau_{el} = \tau_{vib} = \tau_{diss} = 0 \tag{3}$$

The first two conditions, of course, give a flow with frozen dissociation. The latter condition gives the equilibrium flowfield.

Nonequilibrium flow computations are made for the case where dissociation is the only relaxation process ($\tau_{trans} = \tau_{rot} = \tau_{vib} = \tau_{el} = 0, 0 < \tau_{diss} < \infty$), and for the case where dissociation and vibration occur simultaneously and interact with each other ($\tau_{trans} = \tau_{rot} = \tau_{el} = 0, 0 < \tau_{vib}, \tau_{diss} < \infty$).

A model to account for the vibration-dissociation coupling was proposed in Ref. 5. This model accounts for the effect of vibrational relaxation on the dissociation. The models of Treanor and Marrone[11,12] and Heims[13] account additionally for the effect the dissociation has on the vibrational relaxation.

The model of Treanor and Marrone as reported in Ref. 12 has been used for these computations. In this model the effect of the vibrational relaxation on the dissociation is accounted for by the vibrational coupling factor V

$$V \equiv k_d/k_{deq}$$

where k_d is the actual rate constant; k_{deq} is the dissociation rate that would exist with vibrational equilibrium at the local translational temperature.

Treanor and Marrone postulate a probability for dissociation and further assume a Boltzmann distribution in the vibrational mode in writing the vibrational coupling factor. The model contains an adjustable constant U which is taken to be $U = D/6k$ in the numerical computation reported here. D is the dissociation energy and k the Boltzmann constant.

A more consistent treatment of the coupled vibration-dissociation process is given by Keck and Carrier,[15] though for dissociation of a diatomic molecule in an inert background gas. According to this theory vibration dissociation occurs in two steps. The first rapid phase establishes an "almost" Boltzmann distribution in the vibrational mode. This phase, during which dissociation is negligible, gives rise to incubation times.[16] The second phase, which has been treated classically and quantum-mechanically in Ref. 15, is much longer. During this phase the usual phenomenological rate equation is valid, but with rate constants that are depressed below their equilibrium value.[14–17]

Treanor and Marrone's phenomenological model is in qualitative agreement with the findings of Ref. 15; for the present purpose, it is important that this model can be formally applied to the dissociation in pure oxygen, and further that it is still simple enough to be used in flowfield computations.

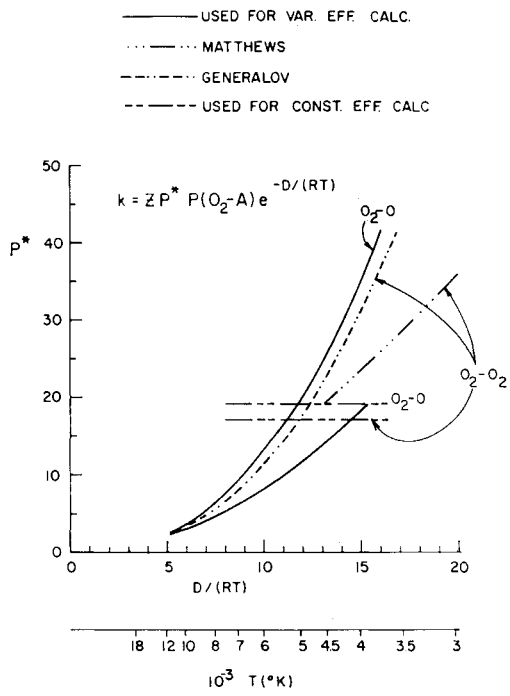

Fig. 4 Relative efficiency P^* as $f(T)$.

Rate Coefficients and Vibrational Relaxation Times

Constant Efficiency Model

The interpretation of the rate constants measured in shock tubes is made difficult because most of the rates are measured under conditions where coupling is important. The so-called pre-exponential factor shows an inverse temperature dependence, which can be caused by nonequilibrium effects in the dissociating molecule.[14,15,19] Such a pre-exponential factor has been found in the experiments by Camac and Vaughan[20] for the dissociation of O_2 in an argon bath. Indeed, their rate coefficient is of the form given by Ref. 14.

In order not to account twice for the coupling, the pre-exponential factor should be removed from the rate expression. This has not been done; as will be seen below, there is an even stronger temperature dependence of the pre-exponential factor for the case of dissociation in pure oxygen for which there is currently no explanation.

The computations done are based on Camac and Vaughan rate constants. In order to apply their results to the dissociation of pure oxygen the relative efficiency of O_2 and O with respect to A has to be known. If the rate coefficient is written in the form

$$k_d(O_2 - O,O_2) = Z_0(O_2 - O,O_2)P^*P(O_2 - A)e^{-D/RT}$$

where $P(O_2 - A)$ is defined by the equation, $k_d(O_2 - A) = Z_0(O_2 - A) \cdot P(O_2 - A)e^{-D/RT}$; then we may consider P^* the efficiency of O_2 and O relative to argon. Z_0 is the bimolecular collision rate for unit concentrations of the reactants. Often, just the ratio of rate constants is termed efficiency. It follows that P^* is proportional to the ratio of the rate constants;

$$P^* = [k_d(O_2 - O,O_2)/k_d(O_2 - A)][(\sigma_{o,o_2}/\sigma_A)(\mu_{o,o_2}/\mu_A)]$$

where σ is the symmetry number and μ is the reduced mass, and where it has been assumed that the mean collision diameter is the same for all collisions. Wray[21] has recommended for use in the low-temperature regime the reaction rate ratios as $A:O_2:O = 1:9:25$. This amounts to taking the efficiency P^* as a constant. The P^* values resulting from this recommendation are shown in Fig. 4 as independent of the temperature.

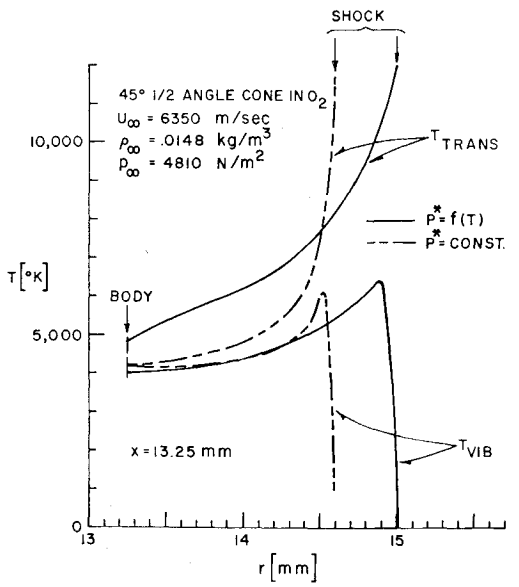

Fig. 5 Theoretical temperature distribution in the shock layer; case 1.

This recommendation has been widely followed in nonequilibrium computations even in the high-temperature regime. Such a constant factor can be explained on the basis of transfer of rotational energy of the colliding molecule into vibrational energy of the dissociating molecule. The computations made with this assumption of constant relative efficiency are labeled "P^* = const" in this report. The vibrational relaxation time for the (O_2 — O_2) collisions in these computations was taken from Camac[20] and extrapolated to the temperatures encountered in these experiments according to the Landau-Teller formula.

Variable Efficiency Model

Measurements of the rate coefficients of pure oxygen show that the relative efficiency P^* is a function of T. For O_2 — O_2 collisions this is demonstrated in Ref. 14. For use in the present computation the relative efficiency P^* is assumed of the form $P^*(O_2 - O_2) \sim C(D/RT)^n$. The constants C and n are determined from the condition that $k_d(O_2 - A)$: $k_d(O_2 - O_2) = 1:9$ for $T = 4{,}000°K$ according to Wray's recommendation, and from the condition that for $T = 7{,}000°K$, $k_d(O_2 - A):k_d(O_2 - O_2) = 1:3$ which is suggested on the basis of Camac and Vaughan's measurements. P^* as a function of T is plotted in Fig. 4. Also plotted are values of P^* based on the rate constants measured by Generalov (3,000–7,000°) and Mathews (3,000–5,000°).

Atomic oxygen has been found highly effective in O_2 — O collisions at low temperatures; however, at high temperatures Wray[18] noticed a drastic decrease in atomic oxygen efficiency, the efficiency approaching that of argon at very high temperatures. Again, assuming $P^* \sim C(D/RT)^n$, C and n are determined from the ratio of reaction constants at 6000°K (Camac and Vaughan)[20] and at 17,000°K according to Ref. 18. The resulting dependence of P^* on T is shown in Fig. 4.

In the vibrational excitation process a similar decrease in efficiency of oxygen molecules relative to argon has been observed by Generalov as reported in Ref. 14. Oxygen molecules are about five times more effective than argon in exciting molecular vibration in the low-temperature regime (<5000°K). At high temperature the efficiency of oxygen decreases and becomes equal to the argon efficiency. The vibrational relaxation time in the computations for variable efficiency were taken accordingly to be the relaxation times for (O_2 — A) collisions, since the major adjustments in vibrational energy occur in the high-temperature part of the shock layer. See Fig. 5 for theoretical temperature distribution in the shock layer. It may be mentioned that[14] extrapolating the relaxation time for pure oxygen according to the Landau-Teller formula leads to relaxation times which are smaller than measured times. The computations made for variable efficiency and the increased vibrational relaxation times are labeled $P^* = f(T)$ in the figures.

It is seen that for both cases of variable and constant efficiency the reaction rates and relaxation times had to be extrapolated and interpolated to a region where no data are available at this time. Most disturbing is the fact that no satisfactory explanation for the strong temperature dependence of the relative efficiencies exists. As will be seen, this has a large effect on the predicted flowfield.

Comparison of Numerical and Experiment Data

Case 1 will be discussed first. Figure 6 shows the shock position and Fig. 7 the shock layer "thickness."

The experimental points plotted are points obtained from several independent measurements of the same interferogram. The shock location in an interferogram is not as clearly defined as for example in a schlieren picture and the different measurements lead to a scatter, which on the scale of Fig. 7 is quite pronounced. It is seen that the equilibrium flow assumption ($\tau_{vib} = \tau_{diss} = 0$) and the nonequilibrium flow assumption with ($\tau_{vib} = 0, 0 < \tau_{diss} < \infty$) yield practically the same shock layer thickness and can hardly be distinguished even on the scale of Fig. 7.

Predictions based on these two models give shock layer thickness 30–40% smaller than experiment. The shock layer thickness for the coupled vibration-dissociation model and $P^* = \text{const}$ gives better agreement with experiment but the thickness is still seen to be about 20–30% too small. Best agreement is reached for the coupled model and $P^* = f(T)$. Shown also in Fig. 7 are the two conical flows resulting from $\tau_{vib} = \tau_{diss} = \infty$ and $\tau_{vib} = 0$, $\tau_{diss} = \infty$. The latter model yields a shock shape which is in as good or better agreement than the equilibrium flow shock shape. Superficial estimate of the flow for the freestream conditions given would suggest an equilibrium flow.

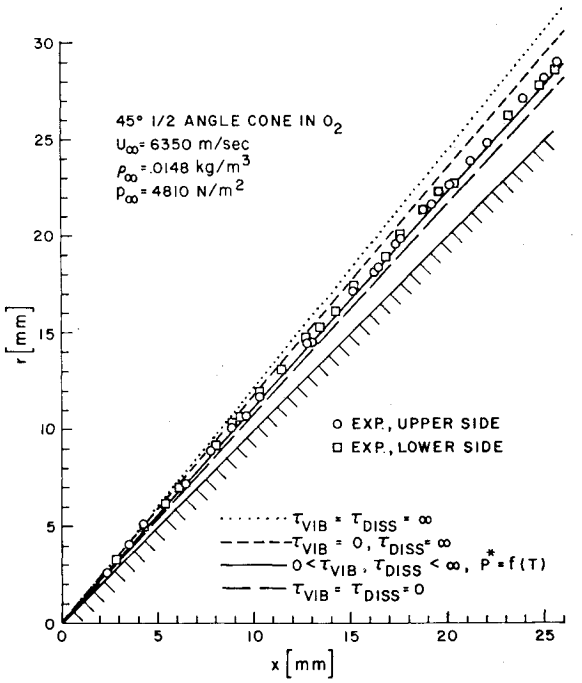

Fig. 6 Comparison of the experimental and theoretical shock position; case 1.

Figure 8 shows the fringe shift δ in units of undisturbed fringe spacing for the various models in comparison with experimental data, for one trace at $x = 16.20$ mm. The fringe shift in the shock layer is plotted as a function of the distance r from the axis to the point for which δ is measured. The fringe shift is computed using experimental refractivities of Ref. 22. These are in good agreement with earlier measurements of Alpher and White.[23]

In the computation the refractivities have been assumed independent of the temperature in the temperature range of the shock layer. In the temperature range of 3000–4500°K this has been shown to be the case for the oxygen atom and molecule by Anderson.[22] There are no experimental data available for the refractivities at higher temperatures. The ratio of specific refractivity at 4000°K to the specific refractivity at 12,000°K of the oxygen atom was found to be 1.00 on the basis of Kramer's dispersion formula and using the best f numbers available. The absolute value thus computed is, however, not in agreement with experimental data.

The refractivities of high-temperature gases are not reliably known at this time, and this introduces an additional uncertainty in the theoretical data. However, the conclusions concerning the shock layer thickness are not affected by the value of specific refractivity; further, the fringe shift computed on the basis of constant refractivity is consistent with the shock data as inspection of Figs. 8 and 9 shows.

In computing the fringe shift the value of the freestream density ρ_∞ is used. Within the experimental error of ρ_∞ the density used in the computation is selected to give at one point on the body, the same fringe shift as the experimental fringe shift at this point. This required a change of freestream density by 10% from the value initially determined from the streak interferogram.† Two sets of data points plotted in Figs. 8 and 9 result from two independent measurements from the same interferogram. The scatter is indicative of the accuracy of measuring the fringe shift. The traces closer to the tip ($x = 10.31$; $x = 11.78$ mm) show the largest scatter. The uncertainty in shock position on the upper side of Fig. 1 where the traces were taken is approximately indicated by the error bars. Figure 8 shows that best agreement with the experimental data is reached for the coupled vibration-dissociation model with $P^* = f(T)$. Figure 9 gives the fringe shift for various traces. The only theoretical curve in this figure is the curve based on the coupled model with variable efficiency.

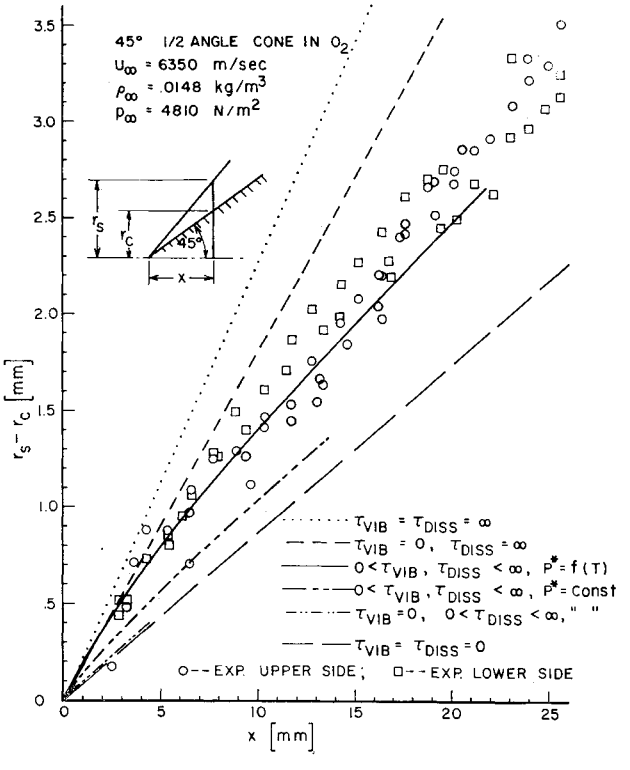

Fig. 7 Comparison of the experimental and theoretical shock layer "thickness;" case 1.

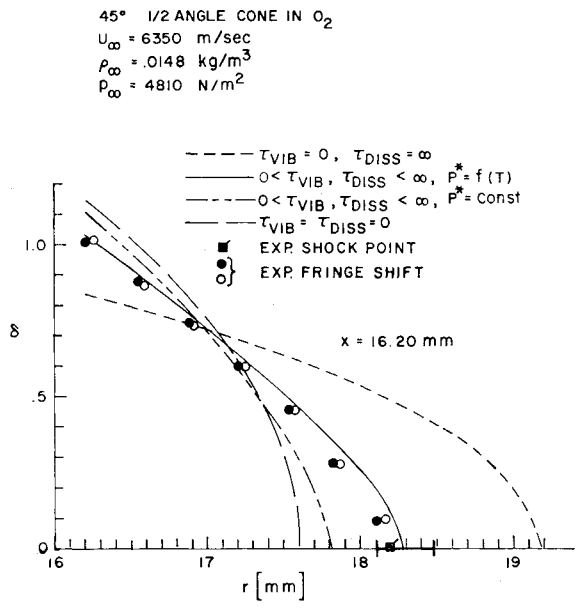

Fig. 8 Comparison of experimental and theoretical fringe shift $\delta(r)$.

For certain conditions, namely if $\Sigma K_i \rho_i / \rho$ is constant in the shock layer (K_i is the specific refractivity and ρ_i the partial density) the fringe shift data can be used to obtain the density distribution. Assuming constant refractivities, the aforementioned condition is fulfilled in this case. The density distribution for the trace at $x = 16.20$ is shown in Fig. 10.

The computation based on the coupled model with variable efficiency $P^* = f(T)$ gives best agreement with experiment. The equilibrium flow computation yields density values about 30% too high. The computation for the uncoupled model ($\tau_{vib} = 0$, $0 < \tau_{diss} < \infty$) was not carried far enough in x to serve for comparison here; however, the traces closer to the tip show that the density distribution very closely duplicates the distribution of the equilibrium flow except for a very steep rise near the shock. The numerical computations for this model were very time-consuming because a small grid size had to be used to handle the strong

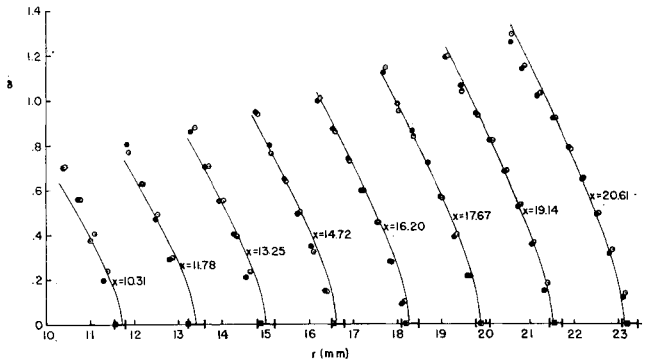

Fig. 9 Comparison of experimental fringe shift $\delta(r)$ with theoretical prediction using $0 < \tau_{vib}, \tau_{diss} < \infty$ and $P^* = f(T)$.

† The numerical predictions given in AIAA Paper 69-136 were based on the uncorrected density. The theoretical data differ from those given here by at most 3%.

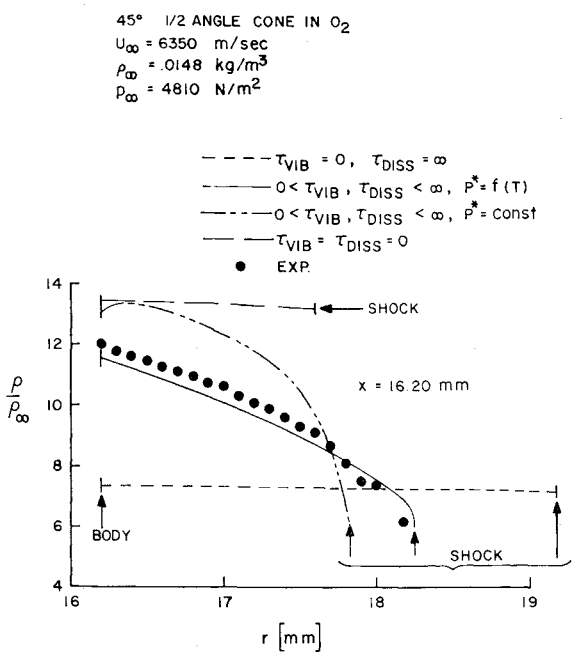

Fig. 10 Comparison of an experimental density trace with theoretical predictions.

gradients in the flow variables near the shock. The coupled vibration-dissociation model with constant efficiency $P^* =$ const gives density distribution about 20% too high.

The experiment for case 2 was done in a modified expansion tube.[24] In this modification the test gas is processed by a reflected shock which heats the test gas high enough to dissociate it. The test gas is subsequently expanded from this dissociated state and nonequilibrium in the freestream may be expected. For the conditions of this experiment the compressibility in the reflected region depends very sensitively on the Mach number of the reflected shock, so that the compressibility in the freestream is uncertain even if no recombination occurs in the expansion process. The nominal value of the freestream compressibility based on the Mach number of the reflected shock and assuming a completely frozen expansion process is $Z_\infty = 1.1$, giving an atom concentration of $C_O = 0.23$ and a molecule concentration of $C_{O_2} = 0.885$, here $C_i = (\rho_i/\rho)/(W_i/W_{O_2})$ and W is the molecular weight. In addition, the vibrational energy is assumed frozen out in the expansion and the freestream vibrational energy is based on the (equilibrium) temperature in the shock reflected region.

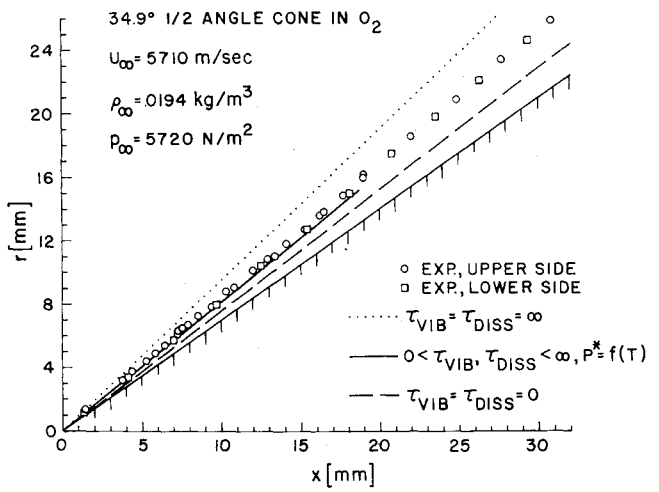

Fig. 11 Comparison of the theoretical and experimental shock shape; case 2.

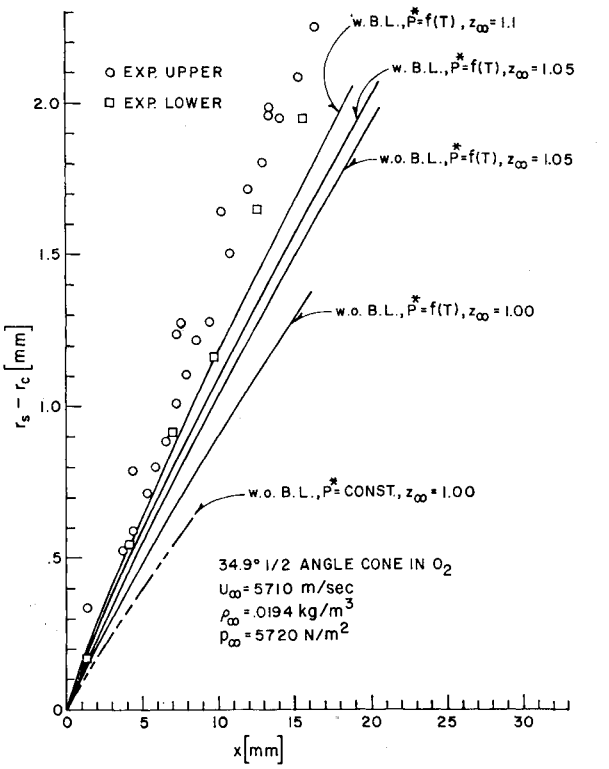

Fig. 12 Comparison of the theoretical and experimental shock layer thickness; case 2.

In the computation of this flow an attempt has been made to correct for the boundary-layer thickness effect. Some of the computation for this case is made for a body which is made up of the cone plus the displacement thickness. The displacement thickness is computed on the basis of an ideal gas of constant γ. For the highly cooled boundary layer the thickness is proportional to the square of the surface Mach number, and is about twice as large in case 2 as in case 1.

Since the resulting body would have a blunted tip a conical forebody has been attached to the tip, which has the largest possible angle consistent with an attached shock and purely supersonic flow for the given freestream Mach number. The conical tip with half angle of 38.5° attaches to the body where the slopes of their generating curves are the same. The combined body is 0.001 mm longer than the original cone. The computed density profiles for this body are found to be essentially the same as for the cone, except displaced radially by the displacement thickness. Figure 11 shows the shock position and Fig. 12 the shock layer thickness. The computations are carried only to 20 mm because at this point the memory capacity of the computing machine was exceeded.

In this case, the effect of vibration-dissociation coupling on the shock layer flow should be reduced, since the maximum temperature in the shock layer is only 8600°K. However, as Fig. 12 shows, the effect of boundary layer becomes noticeable and the freestream dissociation has a large effect on the flowfield. The value of Z_∞ is not well known in this experiment and this should be considered when comparing the experiments and theory plotted in Fig. 12. However, it is seen that the model with variable efficiency gives the best agreement with experiment. Just as in case 1, even this model predicts a shock layer somewhat too small.

Conclusions

Experiments of nonequilibrium flows around cones in oxygen have been compared with numerical prediction. The freestream conditions are such that the flowfield in the shock layer is determined by various overlapping relaxation pro-

cesses. Of these, only the coupling between vibration and dissociation relaxation processes has been considered, although an effect of rotational and possibly translational nonequilibrium must be expected for portions of the shock layers.

The coupling between vibration and dissociation has been treated with a phenomenological model which is simple enough to be used in flowfield computations and still retains the main features of the chemical kinetic process. Best agreement with experiments was obtained for the model that accounted for variable effectiveness of O_2 and O collisions in the excitation of vibration and dissociation. The two effects, namely the vibration-dissociation coupling and the decreased efficiency, appear to be equally important in order to obtain agreement with these experimental results. Possibly, the decreased efficiency effect is a coupling effect also, involving the other degrees of freedom, though it is possible that it is caused by differences between the interaction potentials of the O_2 — A and O_2 — O_2, O complex which becomes more pronounced at the higher temperatures.

There is ample experimental evidence for the decreased efficiency at high temperatures, and indeed the rates used here are based on shock tube data; however, the extrapolation used in the rate constants and vibrational relaxation times used in these computations should be considered with caution, since there is no satisfactory theoretical explanation for the decrease in efficiency.

The usual practice of neglecting coupling effects leads to an inaccurate description of the flowfield. (Additional computations, not reported here, with $\tau_{vib} = 0$ but with $P^* = f(T)$ instead of $P^* = \text{const}$—which are reported here—do not give agreement with experimental data either.) Conditions where coupling becomes important are encountered for situations of practical interest. In this connection it may be mentioned that based on binary scaling the flowfields considered here are representative for flight of a body say of 1 ft diam at 140,000 ft altitude in an oxygen atmosphere at 20,000 fps velocity. In air the analysis of the flowfield under similar conditions is rendered much more difficult because many coupled relaxations occur that are presently not sufficiently understood.

References

[1] Hall, J. G., Eschenroeder, A. Q., and Marrone, P. V., "Blunt-Nose Inviscid Airflows with Coupled Nonequilibrium Processes," *Journal of the Aerospace Sciences*, Vol. 29, No. 9, Sept. 1962, pp. 1038–1051.

[2] Wood, A. D., Springfield, J. F., and Pallone, A. J., "Chemical and Vibrational Relaxation of an Inviscid Hypersonic Flow," *AIAA Journal*, Vol. 2, No. 10, Oct. 1964, pp. 1697–1705.

[3] Spurk, J. H., Gerber, N., and Sedney, R., "Characteristic Calculation of Flowfields with Chemical Reactions," *AIAA Journal*, Vol. 4, No. 1, Jan. 1966, pp. 30–37.

[4] Spurk, J. H. and Bartos, J. M., "Interferometric Measurement of the Nonequilibrium Flow Field Around a Cone," *The Physics of Fluids*, Vol. 9, No. 7, July 1966, pp. 1278–1285.

[5] Hammerling, P., Teare, J. D., and Kivel, B., "Theory of Radiation from Luminous Shock Waves in Nitrogen," *The Physics of Fluids*, Vol. 2, No. 4, July-Aug. 1959, pp. 422–426.

[6] Lin, S. C. and Fyfe, W. I., "Low-Density Shock Tube for Chemical Kinetics Studies," *The Physics of Fluids*, Vol. 4, No. 2, Feb. 1961, pp. 238–249.

[7] Spurk, J. H., "Design, Operation, and Preliminary Results of the BRL Expansion Tube," *Proceedings of the Fourth Hypervelocity Techniques Symposium*, Arnold Air Force Station, Nov. 1965, pp. 111–145.

[8] Spurk, J. H., Knauss, D. T., and Bartos, J. M., "Interferometric Measurement of Nonequilibrium Flow Fields Around Cones and Comparison with Characteristic Calculations," *AGARD Conference Proceedings*, No. 12, Vol. 2, *Recent Advances in Aerothermochemistry*, Harford House, London, 1967, pp. 569–592.

[9] Spurk, J. H. and Gion, E. J., "Impurity Concentration in the Expansion Tube," *AIAA Journal*, Vol. 7, No. 2, Feb. 1969, pp. 346–348.

[10] Herzberg, G., *Spectra of Diatomic Molecules*, 2nd ed., D. Van Nostrand, New York, 1950, p. 92.

[11] Treanor, C. E. and Marrone, P. V., "Effect of Dissociation on the Rate of Vibrational Relaxation," *The Physics of Fluids*, Vol. 5, No. 9, Sept. 1962, pp. 1022–1026.

[12] Marrone, P. V. and Treanor, C. E., "Chemical Relaxation with Preferential Dissociation from Excited Vibrational Levels," *The Physics of Fluids*, Vol. 6, No. 9, Sept. 1963, pp. 1215–1221.

[13] Heims, S. P., "Moment Equations for Vibrational Relaxation Coupled with Dissociation," *Journal of Chemical Physics*, Vol. 38, No. 3, Feb. 1963, pp. 603–606.

[14] Stupochenko, E. V., Losev, S. A., and Osipov, A. I., *Relaxation in Shock Waves*, Springer-Verlag, Berlin, 1967, pp. 258–286.

[15] Keck, J. and Carrier, G., "Theory of Nonequilibrium Dissociation and Recombination," Research Rept. 212, April 1965, AVCO-Everett Research Lab., Everett, Mass.

[16] Brau, C. A., Keck, J. C., and Carrier, G. F., "Transient Phenomena in Dissociation Reactions, I. Theory and Interpretation of Incubation Times," Research Rept. 243, March 1966, AVCO-Everett Research Lab., Everett, Mass.

[17] Osipov, A. I. and Stupochenko, E. V., "Nonequilibrium Energy Distributions over the Vibrational Degrees of Freedom in Gases," *Soviet Physics USPEKHI*, Vol. 6, No. 1, July-Aug. 1963, pp. 47–66.

[18] Wray, K. L., "Shock-Tube Study of the O_2-Ar Rates of Dissociation and Vibrational Relaxation," *Journal of Chemical Physics*, Vol. 37, No. 6, Sept. 1962, pp. 1254–1263.

[19] Widom, B., "Deviations from Thermal Equilibrium Among Reactant Molecules," *Journal of Chemical Physics*, Vol. 34, No. 6, June 1961, pp. 2050–2056.

[20] Camac, M. and Vaughan, A., "O_2 Dissociation Rates in O_2 — Ar Mixtures," *Journal of Chemical Physics*, Vol. 34, No. 2, Feb. 1961, pp. 460–470.

[21] Wray, K. L., "Chemical Kinetics of High Temperature Air," *ARS Progress in Astronautics and Rocketry: Hypersonic Flow Research*, Vol. 7, edited by F. R. Riddell, Academic Press, New York, 1962, pp. 181–204.

[22] Anderson, J. H. B., "An Experimental Determination of the Gladstone-Dale Constants for Dissociating Oxygen," UTIAS TN 105, March 1967, Institute for Aerospace Studies, Toronto, Canada; also Anderson, J. H. B., Osborne, P. K., and Glass, I. I., "Gladstone-Dale Constants for the Oxygen Atom and Molecule," *The Physics of Fluids*, Vol. 10, No. 8, Aug. 1967, p. 1848.

[23] Alpher, R. A. and White, D. R., "Optical Refractivity of High-Temperature Gases. I. Effects Resulting from Dissociation of Diatomic Gases," *The Physics of Fluids*, Vol. 2, No. 2, March-April 1959, pp. 153–161.

[24] Spurk, J. H., Gion, E. J., and Sturek, W. B., "Modified Expansion Tube," *AIAA Journal*, Vol. 7, No. 2, Feb. 1969, pp. 345–346.